JOURNAL OF NEUROTRAUMA 38:1702–1716 (June 15, 2021)

DOI: 10.1089/neu.2020.7309

Adipose Tissue-Derived Mesenchymal Stem Cell Concentrated Conditioned Medium Alters the Expression Pattern of Glutamate Regulatory Proteins and Aquaporin-4 in the Retina after Mild Traumatic Brain Injury

Kumar Abhiram Jha,[1] Jordy Gentry,[1] Nobel A. Del Mar,[2] Anton Reiner,[2] Nicolas Sohl,[3] and Rajashekhar Gangaraju[2]

Abstract

Concentrated conditioned media from adipose tissue–derived mesenchymal stem cells (ASC-CCM) show promise for retinal degenerative diseases. In this study, we hypothesized that ASC-CCM could rescue retinal damage and thereby improve visual function by acting through Müller glia in mild traumatic brain injury (mTBI). Adult C57Bl/6 mice were subjected to a 50-psi air pulse on the left side of the head, resulting in an mTBI. After blast injury, 1 μL ($\sim$100 ng total protein) of human ASC-CCM was delivered intravitreally and followed up after 4 weeks for visual function assessed by electroretinogram and histopathological markers for Müller cell-related markers. Blast mice that received ASC-CCM, compared with blast mice that received saline, demonstrated a significant improvement in a- and b-wave response correlated with a 1.3-fold decrease in extracellular glutamate levels and a concomitant increase in glutamine synthetase (GS), as well as the glutamate transporter (GLAST) in Müller cells. Additionally, an increase in aquaporin-4 (AQP4) in Müller cells in blast mice received saline restored to normal levels in blast mice that received ASC-CCM. *In vitro* studies on rMC-1 Müller glia exposed to 100 ng/mL glutamate or RNA interference knockdown of GLAST expression mimicked the increased Müller cell glial fibrillary acidic protein (a marker of gliosis) seen with mTBI, and suggested that an increase in glutamate and/or a decrease in GLAST might contribute to the Müller cell activation *in vivo.* Taken together, our data suggest a novel neuroprotective role for ASC-CCM in the rescue of the visual deficits and pathologies of mTBI via restoration of Müller cell health.

Keywords: confocal; glutamate; inflammation; mesenchymal; Müller; neurodegeneration

Introduction

Mild traumatic brain injury (mTBI) is the leading cause of vision loss and blindness in military, sports-related injury, and traffic accidents in the United States.[1] In mTBI, pathological alterations to the blood–tissue barrier have been noted in both the brain and retina. Although it is known that breakdown of the blood–retina barrier in mTBI can result in activation of perivascular microglial cells resulting in damage to neuronal cells of the retina,[1,2] the role of Müller cells in the pathology of mTBI requires further elucidation to inform therapeutic approaches to treating this multifaceted disease process. To this end, the exact molecular machinery involved in Müller cell homeostasis in our mTBI model is not investigated.

Injury to retinal Müller glial cells may have an inordinate effect on mTBI visual deficits because they are responsible for the support of retinal neuron synaptic activity by the uptake of glutamate; control of fluid transport in the inner retina by mediating transcellular ion, water, and bicarbonate transport; and the regulation of the tightness of the blood–retinal barrier through end foot processes that surround retinal blood vessels.[3] Consequently, injury to Müller cells following mTBI is expected to result in retinal edema, neuronal cell dysfunction, and subsequent vision loss.[4] These characteristics make Müller cells a vital target in mTBI therapeutics.

A number of excitatory and inhibitory neurotransmitters, including glutamate, mediate the functions of the retinal circuitry in physiological conditions, and several of them are altered in pathological conditions.[5-7] In the retina, glutamate levels are tightly maintained by Müller glial cells by the glutamate-aspartate transporter (GLAST) and glutamine synthetase (GS).[8,9] The initial, prompt clearance of released glutamate from the extracellular space via GLAST is crucial to prevent glutamate-induced neurotoxicity

[1]Department of Ophthalmology, [2]Department of Ophthalmology, Anatomy and Neurobiology, University of Tennessee Health Science Center, Memphis, Tennessee, USA.
[3]Cell Care Therapeutics, Inc., Monrovia, California, USA.

for normal retinal function.[10,11] Apart from glutamate regulation, Müller cells are also involved in water homeostasis and potassium channel conductance in the retina.[12,13] Aquaporin's (AQPs) are responsible for water and ion homeostasis in the retina. AQP4 is expressed in Müller glia in the retina, and their processes closely associate with photoreceptors and retinal neurons. A variety of pathological conditions such as light exposure and diabetic retinopathy have been correlated with altered expression changes in AQP4.[13,14]

Stem cell–derived secretome-based therapies for the treatment of retinal degenerative diseases show promise; however, their exact mechanism of action and the possible cellular targets is unclear.[15] Previously, we demonstrated that intravitreal injection of human adipose tissue–derived mesenchymal stem cell concentrated conditioned medium (ASC-CCM) protects against the visual deficits of mTBI.[16] A single intravitreal injection of ASC-CCM mitigated loss of visual acuity and contrast sensitivity 5 weeks post–blast injury. Interestingly, blast mice showed increased retinal glial fibrillary acidic protein (GFAP) immunoreactivity in Müller cells, indicative of an astrocytic response to the retinal injury, and blast mice that received ASC-CCM showed a prevention of this Müller cell gliosis. Since mesenchymal stem cell–derived biologics acts via multiple mechanisms of action and effect on modulating multiple cell types concurrently,[17] determining the relative effect of ASC-CCM on the different cell types will help to further clarify the function of adipose tissue–derived stem cell (ASC) therapies.

Considering the involvement of Müller cells in the retinal pathology following mTBI, in this study, we hypothesized that ASC-CCM might rescue retinal damage and thereby improve visual function after mTBI by normalizing GS, GLAST, and AQP4 in Müller cells. Using our mTBI mouse model,[1,18] we show that 4 weeks post–blast injury, ASC-CCM not only decreased extracellular glutamate levels back to normal levels but also increased the expression of GS and GLAST back to sham levels, and decreased the expression of AQP4 in blast mice to normal. Our current *in vivo* and *in vitro* studies, taken together with our previous observation of improvement in visual response with ASC-CCM, suggest a novel indirect neuroprotective role for ASC-CCM in the rescue of visual deficits of mTBI via restoration of Müller cells to a normal state.

Methods

ASC culture and conditioned medium preparation

ASC culture and preparation of concentrated conditioned medium were performed as described by us previously.[17] Briefly, ASCs (Lonza, Walkersville, MD; Cat# PT-5006, Lot# 0000535975) were cultured in serum-free media (MEM-alpha) were primed with 20 ng/mL tumor necrosis factor (TNF)α (R&D Systems) and 10 ng/mL interferon γ (R&D Systems) in basal media for 24 h. ASCs were washed to remove cytokines and then cultured in basal media for an additional 24 h, at which point the conditioned media was collected and concentrated $\sim 20\times$ using a 3 kDa molecular weight cutoff Amicon Ultra-15 centrifugal-concentrator and desalted. Aliquots were stored at -80°C and used in assays subsequently.

Blast injury and study groups

All studies with blast injury were performed as described by us recently. Animal studies were approved by the Institutional Animal Care and Use Committee, UTHSC, Memphis, and USAMRMC Animal Care and Use Review Office following the guidelines per the Association for Research in Vision and Ophthalmology Statement for the Use of Animals in Ophthalmic and Vision Research and the Association for Assessment and Accreditation of Laboratory Animal Care guidelines. The mTBI mouse model of male adult 12-week-old C57Bl/6 mice and the preparation of ASC-CCM used in the current study is described previously.[16] Blast injury mice were divided into two groups based on the intravitreal injection: 1) Blast-Saline (Blast-Sal), which received 1 μL of physiological saline into both eyes; and 2) Blast-ASC-CCM, which received 1 μL (~ 100 ng of protein) of cytokine primed ASC-CCM into both eyes. Sham-blast mice that underwent sham injury[1] received 1 μL of saline into both eyes and served as control. All studies described below performed 4 weeks after intravitreal injections.

Electroretinography

Scotopic threshold electroretinogram (ERG) recordings were obtained using the Espion E2 ERG system (Diagnosys LLC, Lowell, MA), as we described previously.[17] Briefly, mice that were dark adapted exposed to different flashes of increasing intensity ranging from 0.0025 to 25 cd/m^2. Each flash repeated five times with appropriate intervals between flashes to generate a- and b-wave amplitudes.

Glutamate assay in the retina

Some mice were euthanized, and their eyes quickly removed. After carefully removing the anterior chamber, the retinal eyecups were scooped out and snap-frozen until analysis. Retinal free glutamate concentration was measured by a glutamate assay kit following the manufacturer's guidelines (ab83389, Abcam). Retinas were homogenized in 100 μL of assay buffer containing Triton-X 100 and centrifuged at 12,000 rpm for 10 min at 4°C. The supernatant was collected and mixed with 100 μL of the reaction mixture containing glutamate assay buffer, glutamate enzyme, and glutamate developer, incubated at 37°C for about 30 min. Following this, the absorbance was measured at 450 nm using Biotek microplate reader. The amount of glutamate in each retina was then quantified against glutamate standard curve.

Tissue preparation and immunohistochemistry

Some mice were euthanized, and their eyes quickly removed. The cornea was cut away, the lens and vitreous were removed, and the eyecups fixed for 4 h in freshly prepared 4% paraformaldehyde at 4°C. Subsequently, the eyecups were cryopreserved in a graded series of sucrose solution and embedded in optimal cutting temperature (Microm-HM 550, Thermo Scientific) at -20°C. About 12-μm thickness of the retina along a dorsal to the ventral axis were placed on to L-poly lysine coated slides and stored at -20°C for further use. Immunohistochemistry (IHC) was used to localize the expression of target proteins. Cryosections were washed three times with 0.1 M phosphate-buffered saline (PBS) and 0.01% Triton-X. Following this non-specific binding sites were blocked with 5% normal serum in 0.1 M PBS for 1 h and then incubated in primary antibodies (Table 1) against GS (dilutions: 1 μg/mL, mouse monoclonal, catalog number:

Table 1. List of Antibodies

Primary Ab	*Dilution for WB*	*Catalogue Number*	*Sources*
Anti-GFAP	1 μg/mL	ZO334	Dako
Anti-GS	1 μg/mL	MAB302	Millipore
Anti-GLAST1	1 μg/mL	ab416	Abcam
Anti-AQP4	1 μg/mL	A5971	Sigma-Aldrich
Anti- β-tubulin	1 μg/mL	MA5-16308	Thermo Fisher Scientific

Ab, antibody; WB, Western blotting; GFAP, glial fibrillary acidic protein; GS, glutamine synthetase; GLAST, glutamate transporter; AQP4, aquaporin-4.

MAB302, Millipore), GLAST (dilutions: 2 μg/mL, rabbit polyclonal, catalog number: ab416, Abcam), or AQP4 (dilutions: 2 μg/mL, rabbit polyclonal, catalog number: A5971, Sigma-Aldrich) for 48 h at 4°C.

After three consecutive washes with 0.1 M PBS-Triton-X, sections were incubated in their respective secondary antibodies (goat anti-rabbit IgG Alexa Fluor 488 or 546 and goat anti-mouse IgG Alexa Fluor 546, dilution: 2μg/mL, Thermo Fisher Scientific) for 2 h at room temperature. Finally, after a brief wash retinal sections were incubated with DAPI for nuclear staining, and examined under a laser scanning confocal microscope (Zeiss LSM 710). Tissue sections without exposure to the primary antibody served as negative controls for immunostaining. The average relative fluorescence units (RFU) per 100,000 μm^2 of the retina for GS, GLAST, and AQP4-immunolabeling were analyzed from at least three sections (from NFL to retinal pigment epithelium [RPE]) per eye by an investigator blinded to the groups.

rMC-1 cell culture

The rMC-1 (Cat#ENW001, Kerafast) were cultured in Dulbecco's Modified Eagle Medium (DMEM) containing L-glutamine and supplemented with 10% of HI-FBS, 100 U/mL penicillin, and 100 ug/mL streptomycin. The cells were incubated in a humidified 5% CO^2 incubator at 37°C. Upon reaching 90%, confluence cells were trypsinized and plated in individual plates for subsequent experiments. For studies involving exposure to glutamate, about 100,000 cells in a well of a 24-well plate were incubated with 0.5 mL basal growth medium and challenged with 100 ng/mL of glutamate for 2 h. For studies involving ASC-CCM, rMC-1 were grown in serum-free media and pre-incubated cells with ASC-CCM (10 μL/0.5 mL) for 4 h before exposing them to glutamate (100 ng/mL) for 24 h.

WST-1 viability assay of rMC-1 glial cells

About 10,000 cells/well of rMC-1 were cultured in a 96-well plate. After 2 h of attachment, cells were washed twice with Dulbecco's PBS (DPBS) and incubated with 2 μL ($\sim$ 200 ng of protein) of ASC-CCM in serum-free DMEM. After 4 h, cells were exposed to different concentrations of glutamate (50, 100, and 200 ng/mL) or H_2O_2 (positive control) for further 24 h in a humidified 5% CO_2 incubator at 37°C. Cell viability was analyzed using WST-1 (TaKaRa; Cat #MK400) dye according to the manufacture guidelines. The colored formazan products were measured at 450 nm and 690 nm using Biotek microplate reader. The cell viability was plotted against glutamate concentration.

Small interfering RNA transfection to reduce GLAST in rMC-1

To knockdown GLAST in rMC-1, cells were seeded at 100000 cells/well of a six-well plate in complete DMEM media. After cell attachment, rMC-1 was transfected with 100 nM of small interfering RNA (siRNA) against GLAST (Thermo Fisher) or negative control siRNA using RNAiMax (Thermo Fisher Scientific, Cat#13778-150) reagent. After 24 h of transfection, rMC-1 was washed with DPBS, exposed to ASC-CCM (20 μL /mL) for 4 h, and challenged with 100 ng/mL of glutamate for a further 24 h. Finally, cells were harvested for gene expression analysis.

Real-time polymerase chain reaction and Western blotting

Both retinal tissue samples from blast injury experiments and rMC-1 cells were processed for RNA and protein for gene and protein expression, respectively. Briefly, after various treatments, RNA was isolated using NucleoSpin® RNA Plus kit (Macherey-Nagel GmbH, Takara Bio USA), following the manufacturers protocol. About 250 ng of total RNA from each sample was converted to complementary DNA (cDNA) using SuperScript III first-strand synthesis supermix (Thermo Fisher Scientific). The resulting cDNA sample served as a template for real-time quantitative polymerase chain reaction (qPCR) using TaqMan probes (Table 2) and accompanying Master Mix (Applied Biosystems, Foster City, CA). The expression levels of target gene transcripts were determined using the 2–DDCt method and normalized to 18S rRNA.

Western blotting for GFAP, GS, GLAST, and AQP4 was performed to analyze the quantitative changes in their expressions among all experimental conditions. The retinal pellet was preserved during RNA isolation for Western Blotting. The pellet was dissolved in protein dissolving buffer (Macherey-Nagel GmbH, Takara Bio USA), supernatant was collected after centrifugation and stored at -800C. Protein concentrations of the samples were estimated by BCA method. About 25 μg of total protein was loaded in each lane, along with protein markers (molecular weight range: 10-250 kDa, Bio-Rad, Hercules, CA, USA) and resolved on a NuPAGE Bis-Tris pre-cast gels (Thermo Fisher Scientific) and transferred to a PVDF membrane. After blocking the membrane for an hour in 5% bovine serum albumin (BSA) in TBST, it was probed with appropriate primary antibodies (Table 1) for 12 h at 4°C. This was followed by incubation with HRP-conjugated secondary antibodies and detection using an enhanced chemiluminescence kit (GE Healthcare, Chicago, IL). Targeted proteins were probed in separate blots. From independent experiments, mean densitometry data were normalized to control using Image-J software and represented as the ratio of the target protein to ubiquitous endogenous β-tubulin control.

Quantification of immunocytochemistry

Immunocytochemistry was performed to study GFAP, GS, GLAST, and AQP4 in rMC-1 cells as described by us recently.[16] Quantification of pixel intensities for various proteins was analyzed from at least five images from different locations per well and expressed as an average of the experimental groups.

Table 2. TaqMan Probes

Genes	*Assay ID*	*Reference sequence*	*Amplicon length*
18S ribosomal RNA (18s rRNA)	Mm04277571_s1	Mm04277571_s1	115
Glutamate aspartate transporter-1(GLAST-1)	Mm00600697_m1	NM_148938.3	71
Glutamine synthetase (GS)	Mm00725701_s1	NM_008131.4	110
Aquaporin-4 (AQP4)	Mm00802131_m1	NM_009700.2	69
Glial fibrillary acidic protein (GFAP)	Mm01253030_m1	NM_001131020.1	64
Glyceraldehydes 3-phosphate dehydrogenase (GAPDH)	Rn01462662_g1	NM_017008.4	90
GFAP	Rn01253033_m1	NM_017009.2	75
GLAST-1	Rn00570130_m1	NM_001289942.1	88
GS	Rn01483107_m1	NM_017073.3	89

Statistical analysis

Data are represented as mean ± standard error of the mean (SEM) among the three experimental groups *in vivo*. Experiments involving rMC-1 cells *in vitro* were performed in duplicates and repeated three times independently. A one-way parametric analysis of variance, followed by *post hoc* Bonferroni test, was performed to compare the data for statistical significance. Analyses were carried out using SPSS 17 (IBM Inc., USA), and $p \leq 0.05$ was considered to be statistically significant.

Results

ASC-CCM ameliorates increased free glutamate in blast injury mice

Previously we have shown that ASC-CCM could suppress increased GFAP expression in Müller glial cells in mTBI mouse retina.[16] To confirm Müller cell activation in this batch of blast injury mice, we measured GFAP messenger RNA (mRNA) by real-time reverse transcription (RT)-PCR and verified finding with Western immunoblots for all groups (Fig. 1). As expected, the GFAP gene expression significantly increased in the Blast-Sal group compared with the Sham-Blast mice retina, with their levels restored by ASC-CCM in blast mice retina (Sham-Blast vs. Blast-Sal; $p < 0.01$ and Blast-Sal vs. Blast/ASC-CCM; $p < 0.04$; $n = 5$-10; Fig. 1A). To confirm the gene expression results, Western blot was performed in all three groups. As shown in Figure 1B, a significant upregulation in GFAP expression in the Blast-Sal group noted as compared with that in Sham-Blast was seen, with a significant decrease in blast mice that received ASC-CCM compared with blast – vehicle mice (Sham-Blast vs. Blast-Sal; $p < 0.001$ and Blast-Sal vs. Blast/ASC-CCM; $p < 0.001$; $n = 4$). Since the glutamate-glutamine cycle is very tightly regulated in the retina to prevent glutamate-induced neurotoxicity, we then measured the extracellular free glutamate levels in all experimental groups. While the sham-blast retinal tissue measured $255.65 \pm 58.74\ \mu$M of glutamate, the free glutamate level was significantly increased in Blast-Sal group ($396.40 \pm 12.33\ \mu$M; $p < 0.032$). Interestingly, blast mice that received ASC-CCM demonstrated $289.37 \pm 21.65\ \mu$M of glutamate, a 1.3-fold significant reduction as compared with blast mice receiving saline ($p < 0.05$; Fig.1C).

ASC-CCM ameliorates decreased GS in blast injury mice

Given that free glutamate levels are increased in blast injury mice retinas and that GS catalyzes the amidation of glutamate to glutamine, we examined the GS expression pattern in all three experimental groups. While GS expression is noted in inner plexiform layer (IPL), inner nuclear layer (INL), outer nuclear layer (ONL), and microvilli of Müller cell processes in Sham-Blast retina (Fig. 2A), the Blast-Sal group demonstrated a decreased GS expression throughout the retina (Fig. 2B). Interestingly, GS

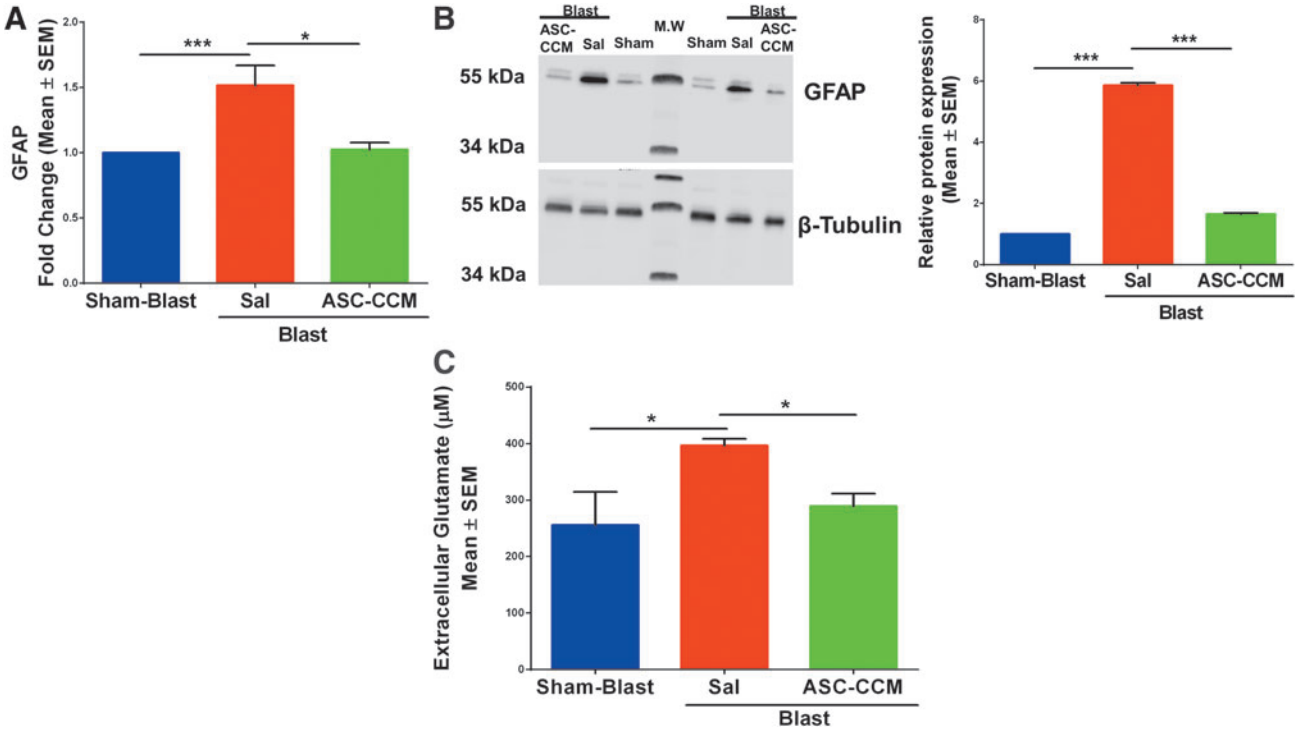

FIG. 1. Intravitreal injection of adipose tissue–derived mesenchymal stem cell concentrated conditioned medium (ASC-CCM) restores the altered glial fibrillary acidic protein (GFAP) expression and extracellular free glutamate levels in blast injury mice. **(A)** Assessment of gene expression by TaqMan quantitative polymerase chain reaction and expressed as fold change normalized to internal control (18s rRNA) in the study groups. Data represent mean ± SEM from $n = 5$-10 animals/group performed in duplicates. *$p < 0.05$; ***$p < 0.001$. **(B)** Representative Western blot showing increased GFAP in the blast-exposed retina and decreased by ASC-CCM intravitreal injection. Mean densitometry data of GFAP protein expression normalized to β-tubulin control using Image-J software. Data represent mean ± SEM from $n = 4$ animals/group. **(C)** Extracellular glutamate measured in retinal extracts by glutamate enzyme-linked immunosorbent assay. Data represent mean ± SEM from $n = 4$-8 animals/group (Sham-Blast vs. Blast-Sal *$p < 0.03$; Blast-Sal vs. Blast/ASC-CCM *$p < 0.05$). Color image is available online.

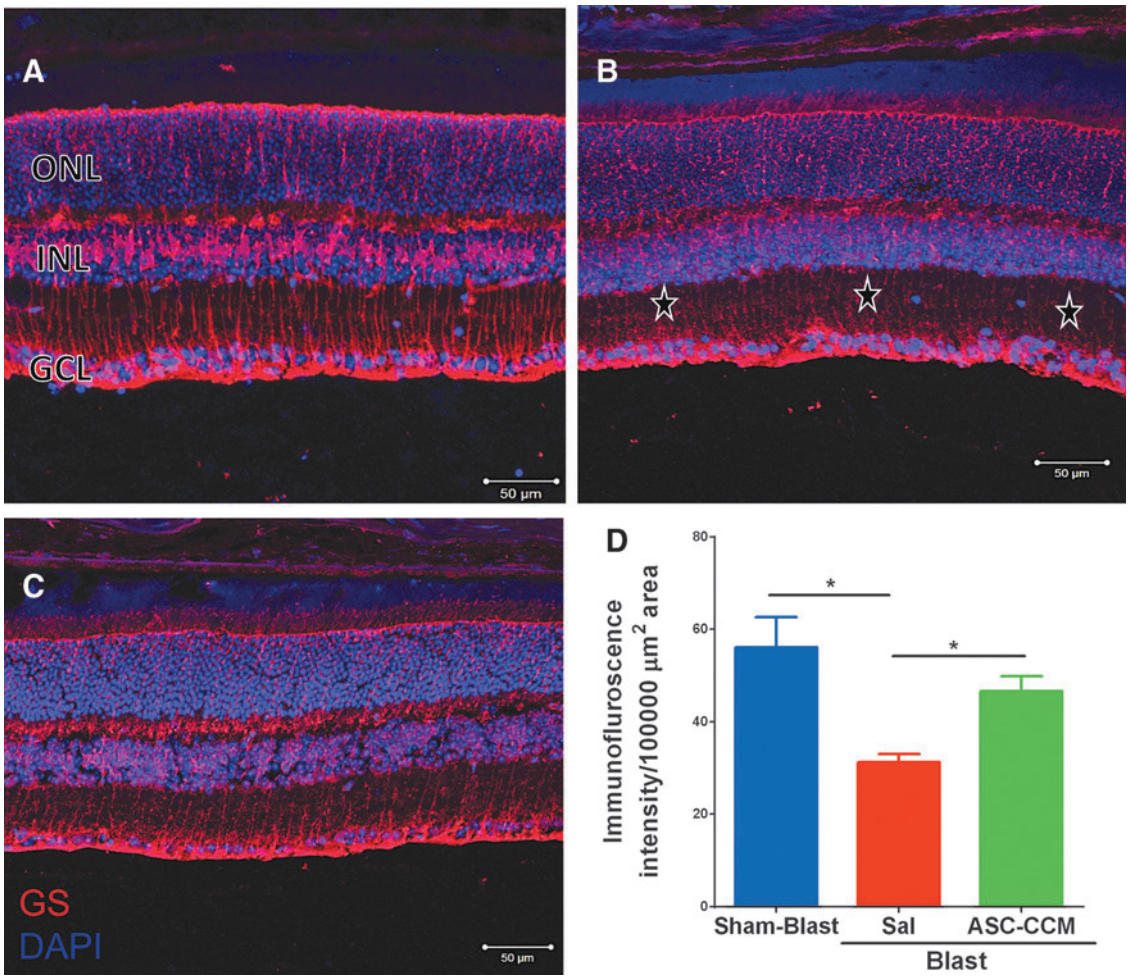

FIG. 2. Decrease in glutamine synthetase (GS) was seen in blast injury retina and improved by intravitreal injection of adipose tissue–derived mesenchymal stem cell concentrated conditioned medium (ASC-CCM). Immunohistological analysis of retinal tissue from all groups 4 weeks post–blast injury. Confocal micrographs showing GS (red) in the retina of Sham-Blast **(A)**, Blast-Sal **(B)**, and Blast/ASC-CCM **(C)** with 4′,6-diamidino-2-phenylindole (DAPI; blue) staining showing different retinal layers (GCL, ganglion cell layer; INL, inner nuclear layer; ONL, outer nuclear layer). **(D)** Image J quantification of GS intensity. * represent areas of significant change. Data represent mean ± SEM from $n = 6$ animals/group (Sham-Blast vs. Blast-Sal $^{**}p < 0.003$, Blast-Sal vs. Blast/ASC-CCM $^{*}p < 0.049$). Scale bar = 50 μm. Color image is available online.

expression was restored to sham blast retina levels in blast injury mice that received ASC-CCM (Fig. 2C). The mean total pixel intensity of GS expression measured from NFL to RPE in normal sham-blast group retina was 56.10 ± 6.56, while the blast group with saline was 31.29 ± 1.78 (mean intensity/100,000 μm^2 area; $p < 0.003$, $n = 6$; Fig. 2D). On the other hand, blast mice with ASC-CCM showed increased GS expression relative to blast–vehicle mice (47.68 ± 2.96 mean intensity/100,000 μm^2 area; $p < 0.049$, $n. = .6$).

To confirm the IHC analysis of GS expression, mRNA levels of GS were assessed by real-time RT-PCR. While the GS expression was significantly decreased in the Blast-Sal mice retina compared with Sham-Blast mice retina, the levels of GS expression were restored by ASC-CCM in the blast-exposed retina (Sham-Blast vs. Blast-Sal, $p < 0.006$ and Blast-Sal vs. Blast/ASC-CCM, $p < 0.019$; Sham-Blast vs. Blast/ASC-CCM, $p > 0.05$; $n = 9$-13; Fig. 5). To confirm the gene expression results, Western blot was performed in all three groups. As shown in Figure 6, a significant reduction in GS expression in the Blast-Sal group noted as compared with that in Sham-Blast was seen, with a significant increase in blast mice that received ASC-CCM compared with blast–vehicle mice (Sham-Blast vs. Blast-Sal, $p < 0.03$; Blast-Sal vs. Blast/ASC-CCM, $p < 0.05$; Sham-Blast vs. Blast/ASC-CCM, $p > 0.05$; $n = 3$-5).

ASC-CCM ameliorates decreased GLAST in blast injury mice

GLAST plays an important role in glutamate metabolism, and it is currently unknown how mTBI could influence its expression in the retina. In the Sham-Blast group retina, widespread expression of GLAST was strongly evident in Müller cell processes passing through the nerve fiber layer (NFL), ganglion cell layer (GCL), IPL, outer plexiform layer (OPL) and ONL in the retina (Fig. 3A). On the other hand, in Blast-Sal group retina, a decreased GLAST expression was observed in Müller cell processes specifically in GCL (star), IPL, INL, ONL, and microvilli of Müller cells as compared with that in Sham-Blast group (Fig. 3B). Interestingly, GLAST expression was restored to sham blast retina levels in blast injury mice that received ASC-CCM (Fig. 3C). The mean total pixel

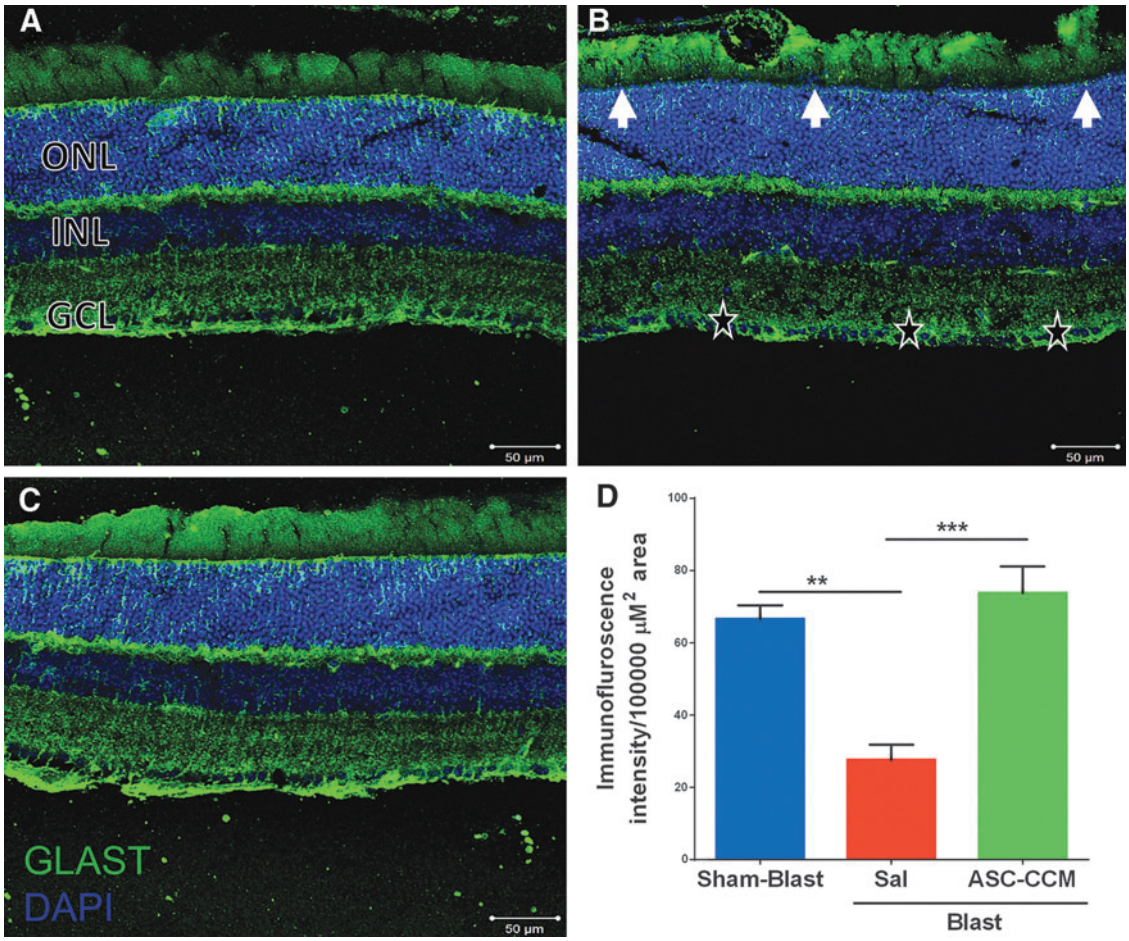

FIG. 3. Decrease in glutamate-aspartate transporter (GLAST) was seen in blast injury retina and improved by intravitreal injection of adipose tissue–derived mesenchymal stem cell concentrated conditioned medium (ASC-CCM). Immunohistological analysis of retinal tissue from all groups 4 weeks post–blast injury. Confocal micrographs showing GLAST (green) in the retina of **(A)** Sham-Blast, **(B)** Blast-Sal, and **(C)** Blast/ASC-CCM with 4′,6-diamidino-2-phenylindole (DAPI; blue) staining showing different retinal layers (GCL, ganglion cell layer; INL, inner nuclear layer; ONL, outer nuclear layer). **(D)** Image J quantification of GLAST intensity. Arrow and * represent areas of significant change. Data represent mean ± standard error of the mean from $n = 4$ animals/group (Sham-Blast vs. Blast-Sal **$p < 0.002$; Blast-Sal vs. Blast/ASC-CCM ***$p < 0.001$). Scale bar = 50 μm. Color image is available online.

intensity of GLAST expression measured from NFL to RPE in normal sham-blast group retina was 66.58 ± 3.77, while for the blast group with saline, it was 27.58 ± 4.28 (mean intensity/100,000 μm^2 area; $p < 0.002$, n = 4; Fig. 3D). On the other hand, blast mice with ASC-CCM showed increased GLAST expression compared with Blast-Sal mice (73.77 ± 7.39 mean intensity/100,000 μm^2 area; $p < 0.001$, $n = 4$). To confirm the IHC analysis of GLAST expression, mRNA levels of GLAST were assessed by real-time RT-PCR.

While the GLAST expression significantly decreased in Blast-Sal compared with Sham-Blast mice retina, the levels of GLAST expression were restored by ASC-CCM in the blast-exposed retina (Sham-Blast vs. Blast-Sal; $p < 0.009$ and Blast-Sal vs. Blast/ASC-CCM- $p < 0.001$; Sham-Blast vs. Blast/ASC-CCM; $p > 0.05$; $n = 9$-13; Fig. 5). To confirm the gene expression at protein levels, Western blot was performed in all three groups. As shown in Figure 6, a significant reduction in GLAST expression in the Blast-Sal group noted as compared with that in Sham-Blast group, with a significant increase in blast mice that received ASC-CCM compared with Blast-Sal mice (Sham-Blast vs. Blast-Sal; $p < 0.04$; Blast-Sal vs. Blast/ASC-CCM; $p < 0.068$ and Sham-Blast vs. Blast/ASC-CCM; $p > 0.05$; $n = 3$-5).

ASC-CCM ameliorates increased AQP4 in blast injury mice

Since the glial water channel protein AQP4 has been associated with edema formation in pathological conditions,[19] we measured AQP4 levels in the retina after mTBI. While the Sham-Blast group retina (Fig. 4A) showed moderate immune reactivity in the GCL, the retinas from the Blast-Sal group demonstrated a widespread expression with intense expression in the end-feet of Müller cells in NFL (star; Fig. 4B). Interestingly, AQP4 expression was restored to sham blast retina levels in blast injury mice that received ASC-CCM (Fig. 4C). The mean total pixel intensity of AQP4 expression measured from NFL to RPE in normal sham-blast group retina was 6.56 ± 1.8, while for the blast group with saline, it was 26.48 ± 4.92 (mean intensity/100,000 μm^2 area; $p < 0.006$, $n = 6$; Fig. 4D). On the contrary, blast mice with intravitreal injection of ASC-CCM showed reduced AQP4 expression (11.08 ± 4.87 mean intensity/100,000 μm^2 area; $p < 0.03$, $n = 6$). To confirm the IHC analysis of AQP4 expression, mRNA levels of AQP4 were assessed by real-time RT-PCR. While the AQP4 expression significantly increased in Blast-Sal group compared with Sham-Blast mice retina,

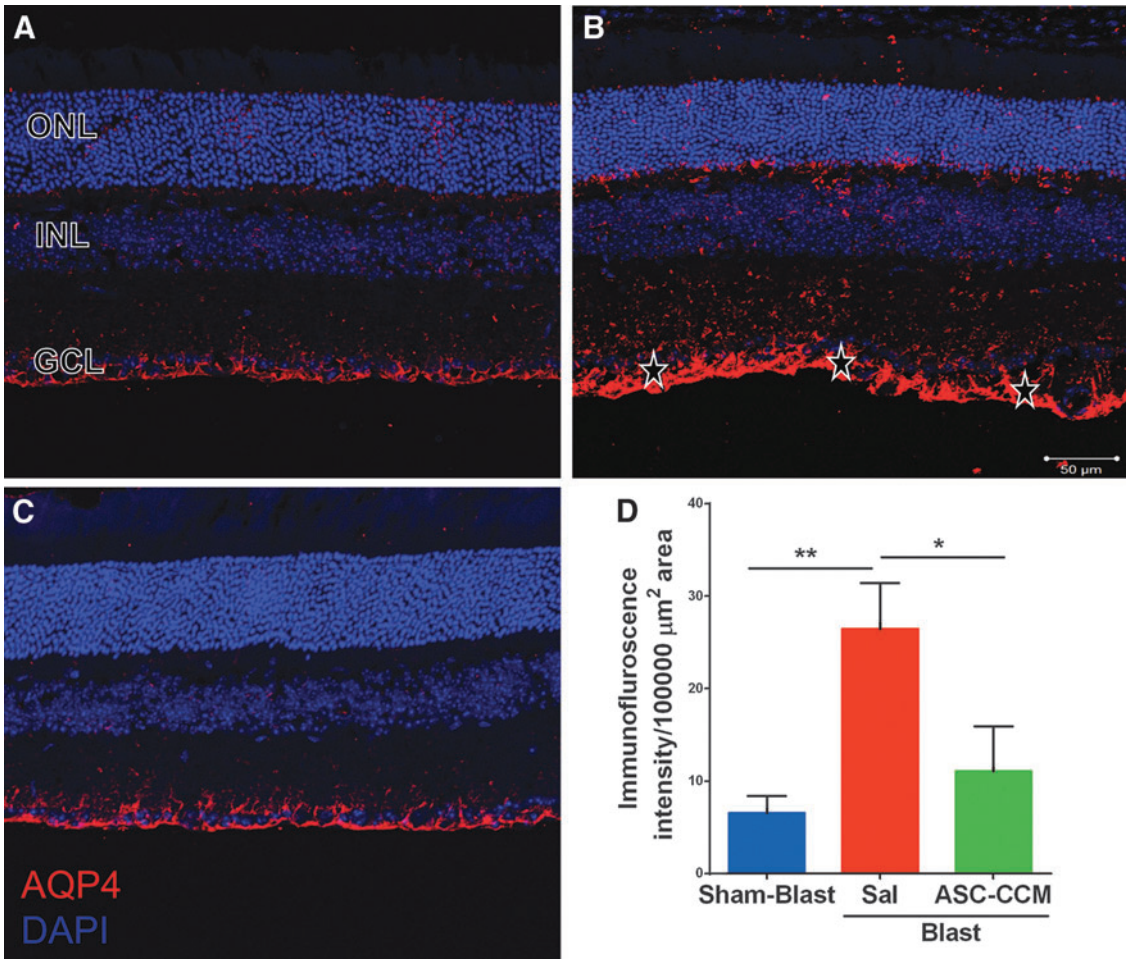

FIG. 4. Increase in aquaporin-4 (AQP4) was seen in blast injury retina and improved by intravitreal injection of adipose tissue–derived mesenchymal stem cell concentrated conditioned medium (ASC-CCM). Immunohistological analysis of retinal tissue from all groups 4 weeks post–blast injury. Confocal micrographs showing AQP4 (red) in the retina of **(A)** Sham-Blast, **(B)** Blast-Sal, and **(C)** Blast/ASC-CCM with 4′,6-diamidino-2-phenylindole (DAPI; blue) staining showing different retinal layers (GCL, ganglion cell layer; INL, inner nuclear layer; ONL, outer nuclear layer). **(D)** Image J quantification of AQP4 intensity. * represents areas of significant change. Data represent mean ± standard error of the mean from $n = 6$ animals/group (Sham-Blast vs. Blast-Sal $^{**}p < 0.01$; Blast-Sal vs. Blast/ASC-CCM $^{*}p < 0.05$). Scale bar = 50 μm. Color image is available online.

the levels of AQP4 expression were restored to sham blast mice levels by ASC-CCM in blast-exposed retina (Sham-Blast vs. Blast-Sal, $p < 0.001$; Blast-Sal vs. Blast/ASC-CCM, $p < 0.001$; and Sham-Blast vs. Blast/ASC-CCM, $p > 0.05$; $n = 9$-13; Fig. 5). To confirm the gene expression at protein levels, Western blot was performed in all three groups. As shown in Figure 6, a significant increase in AQP4 expression in the Blast-Sal group noted was compared with Sham-Blast group, with a significant decrease in blast mice that received ASC-CCM compared with the Blast-Sal mice (Sham-Blast vs. Blast-Sal, $p < 0.04$; Blast-Sal vs. Blast/ASC-CCM, $p < 0.036$ and Sham-Blast vs. Blast/ASC-CCM, $p > 0.05$; $n = 3$-5).

ASC-CCM ameliorates b- and a-wave in blast injury mice

Previously we have shown that ASC-CCM suppresses visual deficits as measured by optokinetic measurements in blast Induced damage.[16] Considering the significant role for Müller cells in the retina that are post-synaptic to the photoreceptors, we measured b-wave and a-wave to determine if changes in glutamate levels affected the ERG. Dark-adapted scotopic ERG responses were recorded from the left eyes of all study groups. With increasing light intensities, an expected increase in b-wave amplitudes could be discerned in all groups, but with a significant reduction noted in the blast-saline mice as compared with sham blast mice across all light intensities ($p < 0.01$). While the b-wave amplitude at 0.25 cd/m^2 light intensity in sham blast group of animals was 396.08 ± 10.14 μV, in blast injury mice that received saline, it was significantly decreased to 297.13 ± 17.35 μV ($p < 0.001$; Fig. 7A). On the other hand, intravitreal injection of ASC-CCM resulted in improvement in the b-wave amplitude across all intensities, with significant improvement from blast-vehicle values noted at 0.25 cd/m^2 (343.38 ± 14.50 μV for the blast-ASC-CCM group; $p < 0.05$), and at 0.025 cd/m^2 (281.98 ± 18.16 μV for the blast-ASC-CCM group; $p < 0.05$). Additionally, blast mice that received intravitreal injection of ASC-CCM were insignificantly ($p > 0.05$) different from sham blast mice suggesting a successful intervention. Similar to the b-wave, a-wave amplitude at 25 cd/m^2 flash light intensity in sham blast group of animals were -308.26 ± 15.35 μV, which was significantly increased to -242.4 ± 15.58 μV in blast injury mice that

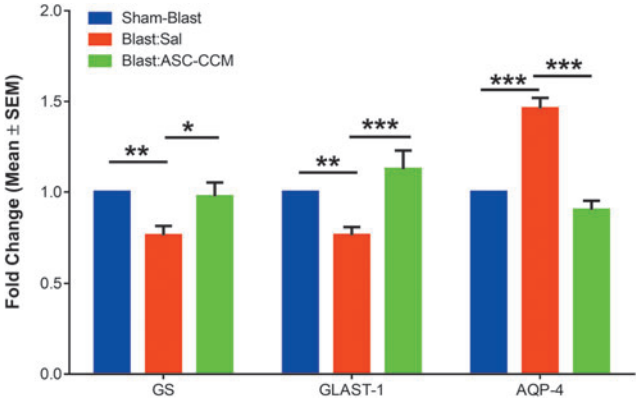

FIG. 5. Intravitreal injection of adipose tissue–derived mesenchymal stem cell concentrated conditioned medium (ASC-CCM) restores the altered retinal gene expression of glutamine synthetase (GS), glutamate-aspartate transporter (GLAST), and aquaporin-4 (AQP4) in blast injury mice. Assessment of gene expression by TaqMan quantitative polymerase chain reaction and expressed as fold change normalized to internal control (18s rRNA) in the study groups. Data represent mean ± standard error of the mean (SEM) from $n = 9$–13 animals/group performed in duplicates. GS (Sham-Blast vs. Blast-Sal $^{**}p < 0.006$, Blast-Sal vs. ASC-CCM $^{*}p < 0.02$); GLAST (Sham-Blast vs. Blast-Sal $^{**}p < 0.009$, Blast-Sal vs. Blast/ASC-CCM $^{***}p < 0.001$) and AQP4 (Sham-Blast vs. Blast-Sal $^{***}p < 0.001$, Blast-Sal vs. Blast/ASC-CCM $^{***}p < 0.001$). Color image is available online.

received saline ($p < 0.04$; Fig. 7B) (meaning it was impaired in blast-saline mice, given that the a-wave is negative-going). On the other hand, intravitreal injection of ASC-CCM resulted in significant improvement in a-wave amplitude at 25 cd/m^2 (299.93 ± 14.00 μV for the blast-ASC-CCM group, $p < 0.02$).

ASC-CCM and glutamate does not affect Müller cell viability

To better understand the role of Müller cell in blast injury mice, rMC-1 cells were assessed *in vitro* for their morphology and viability with glutamate in the presence or absence of ASC-CCM. Neither glutamate (100 ng/mL) nor ASC-CCM treatments altered the morphology of rMC-1 cells (Fig. 8B, 8C). Cell viability studies performed with WST-1 in rMC-1 cells demonstrated expected cleavage of the tetrazolium salt to formazan by cellular mitochondrial dehydrogenase that remained unaffected across all doses of glutamate, with the highest dose showing a marginal decrease in cell viability; however, the data did not reach statistical significance (Fig. 8D). Additionally, those cells that were challenged with glutamate and pre-incubated with ASC-CCM also did not show an effect on the rMC-1 cell viability. Cells incubated with 160 μM H_2O_2, a known inducer of oxidative stress, served as a positive control in the experiment, demonstrating a significant reduction in the cell viability.

ASC-CCM alleviates glutamate-induced changes in GFAP, GLAST, and GS in Müller glia

To establish the direct therapeutic role of ASC-CCM on Müller cells, we next assessed glutamate-induced excitotoxicity on Müller cell markers *in vitro.* To this end, we utilized rMC-1 cells treated with glutamate (100 ng/mL) with or without ASC-CCM for 24 h in serum-free conditions to assess GFAP, GLAST, and GS expression. While the immunofluorescence staining of GFAP appeared more intense in glutamate exposed cells compared with that of untreated control cells, those cells pre-incubated with ASC-CCM and exposed to glutamate showed near-normal expression pattern (Fig. 9A-C). These findings were corroborated by mRNA expression, with a nearly 2-fold increase in GFAP expression with

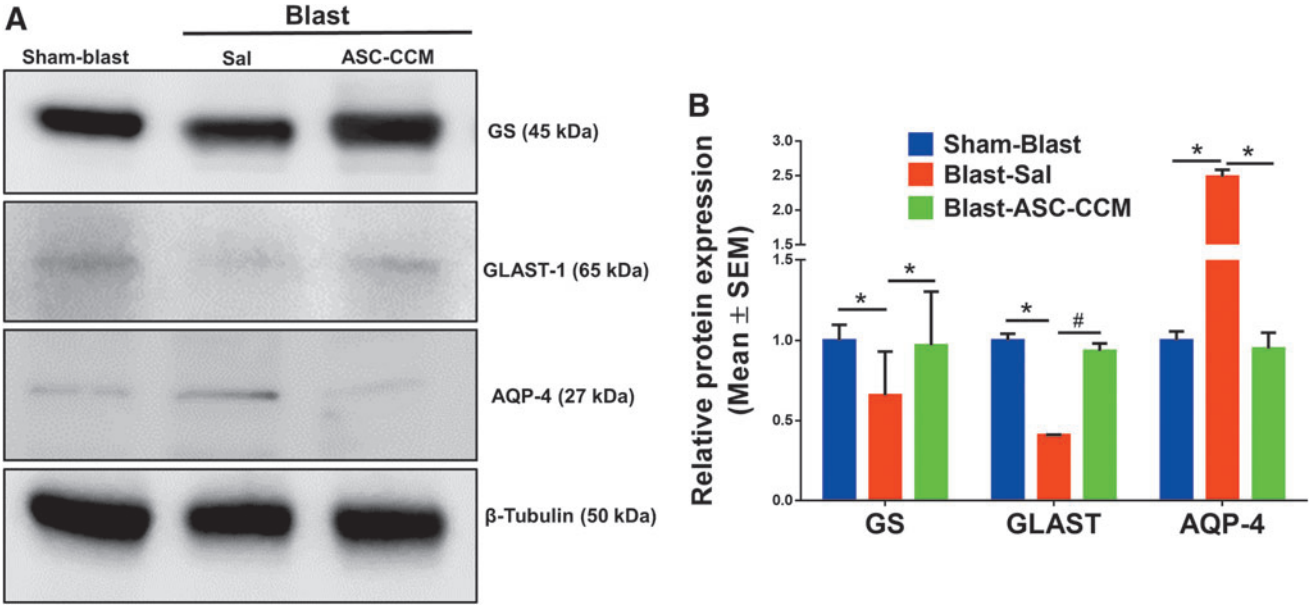

FIG. 6. Intravitreal injection of adipose tissue–derived mesenchymal stem cell concentrated conditioned medium (ASC-CCM) restores the altered protein expression of glutamine synthetase (GS), glutamate-aspartate transporter (GLAST), and aquaporin-4 (AQP4) in blast injury mice. **(A)** Representative Western blot showing decreased GS, GLAST, and increased AQP4 in the blast-exposed retina and improved by ASC-CCM intravitreal injection. **(B)** Densitometry analysis normalized with β-Tubulin. Data represent mean ± standard error of the mean (SEM) from $n = 3$-5 animals/group. GS (Sham-Blast vs. Blast-Sal $^{*}p < 0.03$, Blast-Sal vs. Blast/ASC-CCM $^{*}p < 0.05$); GLAST (Sham-Blast vs. Blast-Sal $^{*}p < 0.03$, Blast-Sal vs. Blast/ASC-CCM $^{*}p > 0.05$) and AQP4 (Sham-Blast vs. Blast-Sal $^{*}p < 0.04$, Blast-Sal vs. Blast/ASC-CCM $^{*}p < 0.03$). Color image is available online.

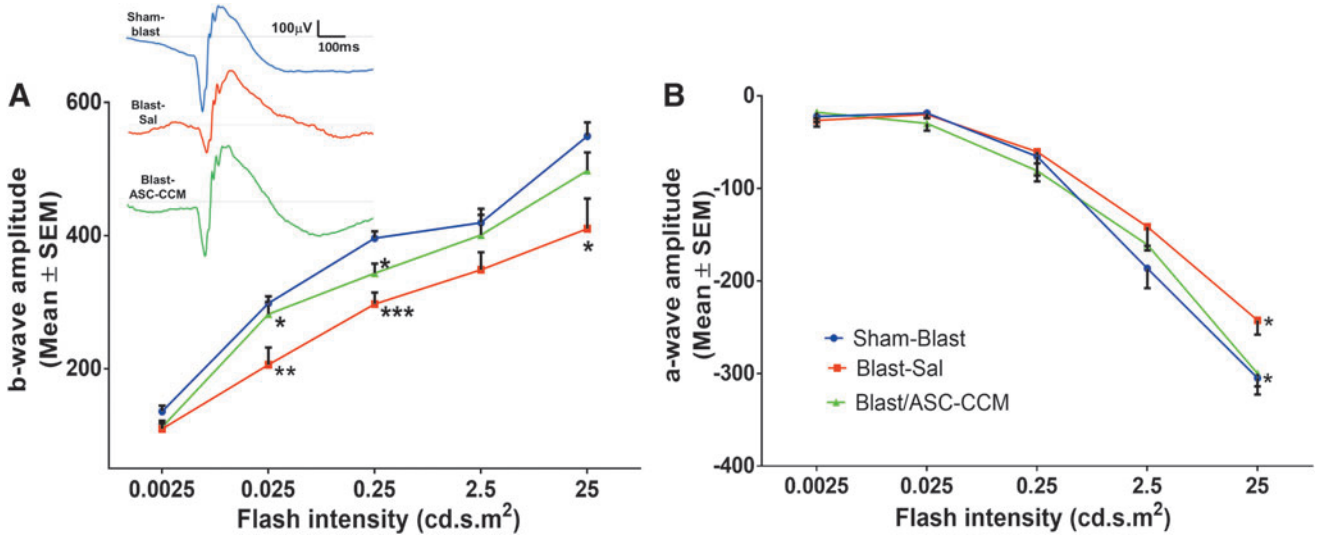

FIG. 7. Intravitreal injection of adipose tissue–derived mesenchymal stem cell concentrated conditioned medium (ASC-CCM) improves retinal function in blast injury mice. **(A)** b-wave amplitude measurement in mice at various flash intensities in the left eye. Inset showing representative electroretinogram tracings from each of the groups. **(B)** a-wave amplitudes from the left eye. Data represent combined mean ± standard error of the mean (SEM) from $n = 5$-8 animals/group. Sham-Blast vs. Blast-Sal ***$p < 0.001$; **$p < 0.01$. Blast-Sal vs. Blast/ASC-CCM *$p < 0.05$. Sham-Blast vs. Blast/ASC-CCM insignificant across all intensities. Color image is available online.

glutamate exposure ($p < 0.02$) and a significant reduction in the case of cells pre-incubated with ASC-CCM and exposed to glutamate compared with cells incubated with glutamate alone ($p < 0.01$; Fig. 9D). While the levels of GS did not differ with exposure to glutamate as assessed by both immunofluorescence (Fig. 9E-G) or real-time RT-PCR (Fig. 9H), the levels of GLAST were significantly reduced in cells exposed to glutamate as assessed by both immunofluorescence (Fig. 9I-K) or real-time RT-PCR, with a significant amelioration with ASC-CCM ($p \leq 0.01$; Fig. 9L).

ASC-CCM alleviates glutamate-induced changes in AQP4 in Müller glia

Since the glial water channel protein, AQP4, was noted to be increased in blast mice, we measured AQP4 expression in rMC-1 cells upon exposure to glutamate in the presence or absence of ASC-CCM. While the expression of AQP4 is very low in untreated control cells (Fig. 10A), its expression as assessed by the immunofluorescence staining demonstrated a robust expression in cells exposed to glutamate as compared with that of untreated control cells (Fig. 10B). On the other hand, those cells pre-incubated with ASC-CCM and exposed to glutamate showed near-normal expression pattern of AQP4 (Fig. 10C). The mean total pixel intensity of AQP4 expression in control group cells was $1.56 \pm 0.2\ \mu m^2$ while the rMC-1 cells exposed to glutamate was $3.59 \pm 0.4\ \mu m^2$ ($p < 0.01$; $n = 6$). On the other hand, rMC-1 cells pre-incubated with ASC-CCM and challenged with glutamate showed reduced AQP4 expression ($2.01 \pm 0.2\ \mu m^2$; $p < 0.01$, $n = 6$; Fig. 10D).

ASC-CCM alleviates glutamate-induced gliosis through actions on GLAST in Müller glia Since we noted that Glutamate exposure reduces the GLAST expression in rMC-1 cells, we asked if GLAST regulates the expression of GFAP and thus might contribute to the Müller gliosis observed *in vivo.* To test this hypothesis, we first transfected rMC-1 cells with a GLAST siRNA or a scrambled control siRNA for 24 h and then exposed to glutamate (100 ng/mL) with or without ASC-CCM for further 24 h (Fig. 11A) and measured the levels of GFAP. First, we confirmed that GLAST siRNA is indeed able to knock down GLAST in rMC-1 cells in the presence or absence of glutamate ($p < 0.001$; Fig. 11B). While the GLAST siRNA transfection resulted in a 2-fold increase in GFAP levels (as compared with control siRNA, $p < 0.001$; Fig. 11C), no further additive increase noted upon exposure to glutamate (as compared with control siRNA, $p < 0.001$; Fig. 11C). Interestingly, those cells pre-incubated with ASC-CCM with and without exposure to glutamate demonstrated a significant reduction in GFAP levels (as compared with GLAST siRNA, $p < 0.05$; Fig. 11C). Surprisingly, GS expression was only marginally upregulated GS in cells treated with GLAST siRNA transfection ($p < 0.04$; Fig. 11D) and remained unaffected with ASC-CCM. Taken together, this suggests that ASC-CCM directly affects GLAST to normalize GFAP in the Müller cells.

Discussion

Our previous studies have demonstrated the beneficial effects of concentrated conditioned medium from cytokine-primed ASC in the mTBI mouse model through neurovascular modulation via decreased microglial and endothelial activation.[16,17] In this study, we show that ASC-CCM may impart its neuroprotective effects via regulating Müller cells. The retinal tissues assessed here at 4 weeks post–blast injury demonstrates adverse changes in Müller cell-related markers, such as increased extracellular glutamate levels with a decreased expression of GS and GLAST, and an increase in the expression of AQP4 in blast mice. Additionally, Müller cells *in vitro* demonstrated a similar decrease in GLAST with increased GFAP upon exposure to glutamate. Interestingly, a single intravitreal injection of ASC-CCM into the blast injury mice ameliorated these glutamate-and Müller cell-related abnormalities, and this action depends, at least in part, on the presence of GLAST, based on our studies in Müller cells *in vitro.*

Prior studies have shown that the TBI model used here does develop retinal thinning, loss of neuronal cells in the retinal ganglion cell layer and loss of axons in optic nerve suggesting

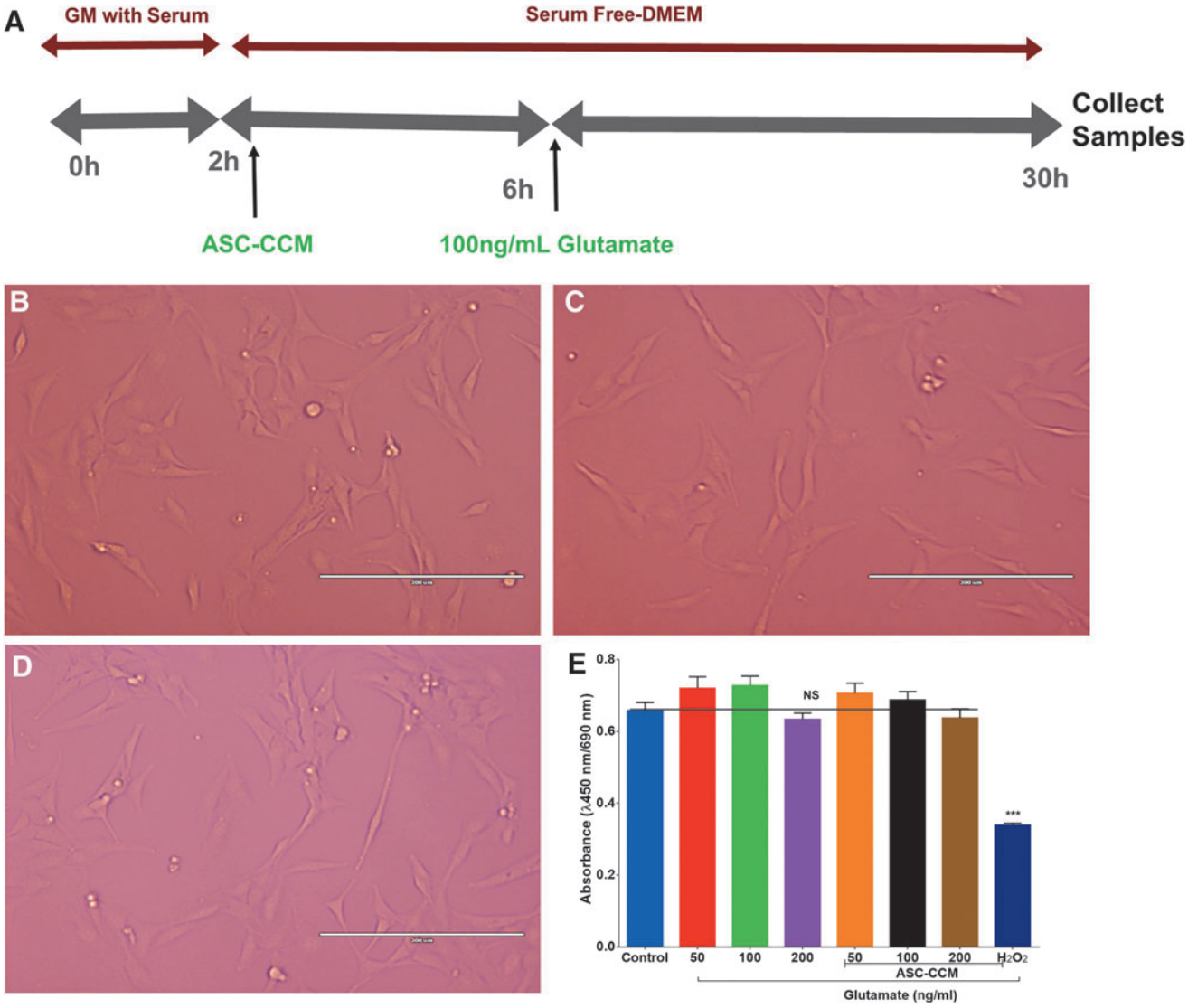

FIG. 8. Adipose tissue–derived mesenchymal stem cell concentrated conditioned medium (ASC-CCM) and glutamate do not affect Müller cell viability *in vitro*. **(A)** The schematic representation of pre-treatment of ASC-CCM and glutamate exposure in rMC-1. **(B-D)** Representative phase-contrast images of rMC-1 cells with no gross morphological changes across all groups. Scale bar = 200 μm. **(E)** The rMC-1 cell viability, as measured with WST-1 with an increasing dose of glutamate in the presence or absence of ASC-CCM. H_2O_2 served as a positive control. Color image is available online.

significant retinal neurodegeneration in blast mice.[1,16,20] Taken together with our previous and present observation of improvement in visual response with ASC-CCM after TBI, our current *in vivo* and *in vitro* studies suggest a novel neuroprotective role of Müller cell modulation in the ASC-CCM rescue of visual deficits of mTBI. Stem cell–derived biologics acting via multiple mechanisms of action and effecting on modulating multiple cell types concurrently may likely overcome the limitations of those therapeutics that modulate a single gene/protein-based signaling pathway for better restoration of endogenous tissue function.

Disruption/damage to the retinal cells in a variety of retinal degenerative diseases is known to alter the metabolic association of the cells within the retina, influencing the retinal neurotransmitter pool.[21] A number of excitatory and inhibitory neurotransmitters are implicated in mediating the functions of retinal circuitry. Specifically, Müller cells play a major role in the recycling of neurotransmitters that drive glioneuronal interactions via their membrane-associated amino acid transmitters such as glutamate, γ-aminobutyric acid, and glycine.[22] Since the normal function of Müller cells depends on the clearance of tightly regulated synaptic glutamate, an accumulation of glutamate interferes with excitatory synapses and contribute to neurotoxicity. In accordance with the current studies, the increase in retinal glutamate after mTBI is likely to contribute to the observed neurodegeneration in the model through disrupted glioneuronal interactions. In certain retinal pathologies as in ischemia, excessive accumulation of glutamate in the extracellular compartment is a strong factor in necrosis, as well as apoptosis in neighboring cells.[23] In line with these observations, previously we have shown a loss of neuronal cells in the GCL in mTBI and a significant rescue with ASC-CCM.[16]

Müller cells express the glutamate/aspartate transporter, GLAST, which is the predominant transporter for the removal of glutamate within the extracellular space of the retina.[8] The initial, prompt clearance of released glutamate from the extracellular space via

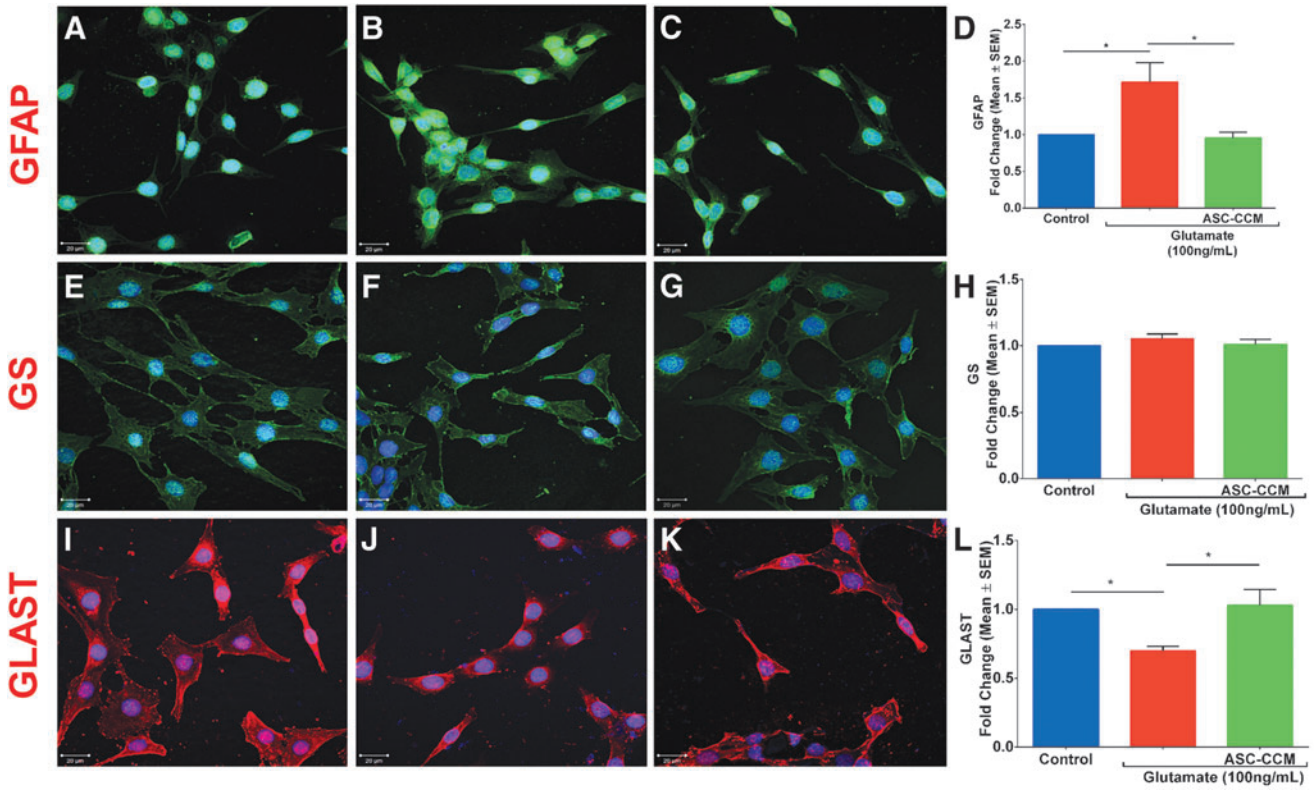

FIG. 9. Adipose tissue–derived mesenchymal stem cell concentrated conditioned medium (ASC-CCM) alleviates glutamate induced changes in glial fibrillary acidic protein (GFAP) and glutamate-aspartate transporter (GLAST) in Müller glia. Confocal immunofluorescence micrographs of rMC-1 cells in control (**A, E,** and **I**), glutamate exposed (**B, F,** and **J**) and glutamate/ASC-CCM (**C, G,** and **K**) groups. (A-C) GFAP (green); (E-G) glutamine synthetase (GS; green) and (I-K) GLAST (red). 4′,6-Diamidino-2-phenylindole (blue) shows nuclear staining. Scale bar = 20 μm. Assessment of gene expression by TaqMan quantitative polymerase chain reaction (qPCR) and expressed as fold change normalized to internal control (glyceraldehyde 3-phosphate dehydrogenase). (D). GFAP, (H). GS and (L) GLAST. Data represent mean ± standard error of the mean (SEM) from $n = 3$ independent assessments/group. *$p < 0.05$. Color image is available online.

GLAST is crucial for normal retinal function as the malfunction of this transport results in increased neurotoxic extracellular glutamate.[10,11] The levels of GLAST in a variety of retinal diseases have been shown to be decreased, including diabetic retinopathy,[24] experimental glaucoma,[25] corticostriatal, and fimbria-fornix lesions,[26] and in the brains of rats after controlled cortical impact-induced TBI coinciding with the excitotoxic damage to the retina.[27] In accordance with these observations, retinal tissue expression of GLAST in blast injury mice was significantly reduced specifically in Müller cell processes in GCL to ONL and microvilli of Müller cells, perhaps contributing to the accumulation of extracellular glutamate and the excitotoxic neuronal damage after TBI. Additional studies involving the siRNA knockdown of GLAST in Müller cells confirm similar observations with increased GFAP expression. In support of this, in astrocytes, GLAST directly interacts with the GFAP cytoskeleton to play an essential role in glutamate homeostasis.[28] Interestingly, Müller cells pretreated with ASC-CCM and challenged with GLAST siRNA demonstrated a substantial recovery in GLAST levels with a concomitant decrease in GFAP, suggesting a direct role for ASC-CCM in altering GLAST and thus contributing to the beneficial effect in mTBI.

Glutamine synthetase (GS), an enzyme located exclusively in Müller cells, converts glutamate to harmless glutamine and works in concert with GLAST.[9] While the expression level of GS appears to be regulated by the availability of its substrate, glutamate, a variety of experimental conditions have shown that exogenous corticosterone can induce GS synthesis in various tissues, including the embryonic chick retina.[10] Although a few studies have found the GS level to increase after cerebral ischemia in experimental rats,[29] a variety of degenerative retinal conditions demonstrated a significant reduction in GS levels.[30] The consorted increase in extracellular glutamate with a decrease in GS warrants further examination; however, the observation that a single intravitreal injection of ASC-CCM normalizes GS in blast injury retina strongly suggests its therapeutic effects via Müller cells. In line with these observations, a previous study involving subretinal transplantation of human umbilical cord tissue–derived cells or their paracrine factors in a purified neuronal culture system demonstrated similar benefits as ASC-CCM.[31,32]

The upregulation of GFAP expression in glial cells is a primary indicator for stress/gliosis in a variety of retinal diseases including light damaged retinas,[33] ischemia and phototoxicity,[34,35] as well as other pathological situations.[36,37] The elevation of GFAP likely due to the hypertrophied nature of the Müller cells forms a barrier around the region of a damage blocking the regeneration of damaged axons and synapses.[38] Müller cell gliosis, similarly to astrogliosis in the central nervous system, is also accompanied by tissue remodeling involving extracellular matrix and changes in several growth factors and inflammatory signaling mechanisms including epidermal growth factor, fibroblast growth factor, TNF-α, ciliary neurotrophic factor, and bone morphogenetic protein among others.[39,40] Toward this end, we have recently shown differential expression of a variety of genes

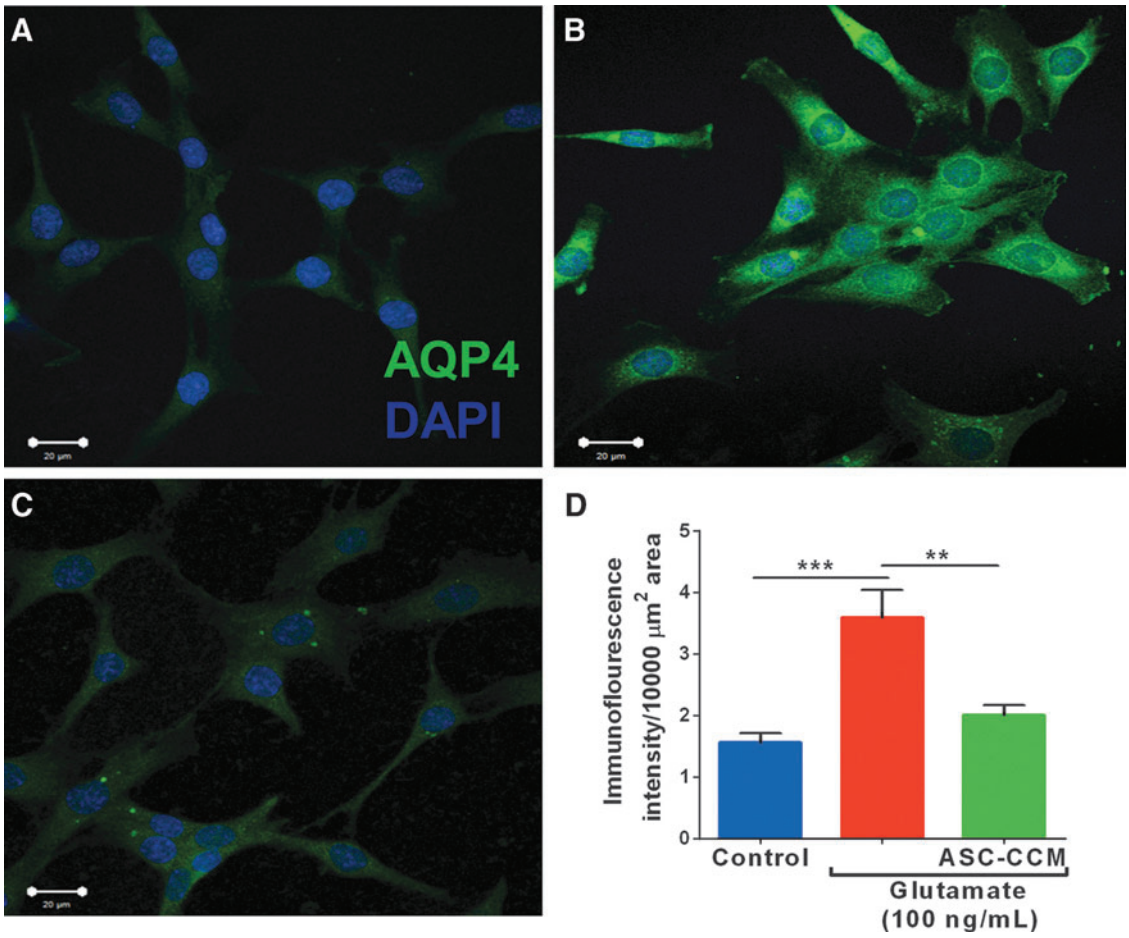

FIG. 10. Adipose tissue–derived mesenchymal stem cell concentrated conditioned medium (ASC-CCM) alleviates glutamate induced changes in aquaporin-4 (AQP4) in Müller glia. Confocal immunofluorescence micrographs of rMC-1 cells in control (A), glutamate exposed (B), and glutamate/ASC-CCM (C) groups. (D). Image J quantification of AQP4 immunofluorescence intensity in rMC-1cells. Data represent mean ± standard error of the mean from $n = 3$ biological replicates /group. ***$p < 0.001$; **$p < 0.004$). Color image is available online.

involved in neuroinflammation, neurotransmission, metabolism, neuroplasticity, development and aging, and neuron-glia interactions in blast injury compared with sham blast, with a significant amelioration with ASC-CCM.[17] Future studies beyond the scope of the current study need to explore cell signaling pathways to understand the neuro-glia interaction in mTBI better.

Aquaporins (AQPs) are integral membrane proteins present throughout the ocular system. Among the variety of AQPs, ocular expression of AQP0, 1, 3, and 5 are predominantly expressed in the cornea, lens, and ciliary epithelium, while AQP4 is exclusively associated with Muller cells.[19] AQP4 is responsible for water and ion homeostasis in the retina.[41] In accordance with this, the level of expression of AQP4 is intimately linked to the formation and resolution of the brain and retinal edema.[42,43] Based on our observation of increased AQP4 in our mTBI model, it is conceivable that increased AQP4 might contribute to the increased edema and thus might contribute to the observed neurodegeneration. Our observations are also in agreement with many pathological conditions, such as light exposure, diabetic retinopathy as well as in a rat model of whole body blast overpressure model that have shown altered expression of AQP4.[13,14,44] Since AQP4 levels are elevated in several pathological conditions, there is also evidence that deletion of AQP4 is neuroprotective as observed in ischemia model of retinal degeneration[45] or intravitreal injection of selective AQP4 inhibitor, 2-(nicotinamide)-1,3,4-thiadiazole (TGN-020) in the diabetic retina.[43] In accordance with these observations, our findings from *in vivo* and *in vitro* studies showed that the intravitreal injection of ASC-CCM could be a potential therapy to suppress neurodegeneration in mTBI through AQP4. While reducing the levels of AQP4 might be beneficial in certain models, it might be a double-edged sword since AQP4 has also been shown to involve in neural signal transduction in the retina due to its association with Muller and neighboring excitable bipolar cells as noted by the impaired visual signal transduction in AQP4 null mice.[46] Additionally, AQP4 null mice also demonstrated altered glutamate levels and affected the expression pattern of GLAST and GS in light damage conditions.[47] Considering these observations, a careful regulation of both AQP4 and glutamate signaling as observed with ASC-CCM, might provide an added advantage.

In conclusion, our findings reveal novel glial mechanisms involved in the benefit of intravitreal ASC-CCM for the retinal injury after mTBI (Fig. 12). Our findings suggest that ASC-CCM provides signals that support homeostatic Müller cell function via glutamate uptake and breakdown to protect retinal synapses that are critical for maintaining vision. Further, our findings suggest that AQP4 signaling is also important for retinal function in mTBI. These

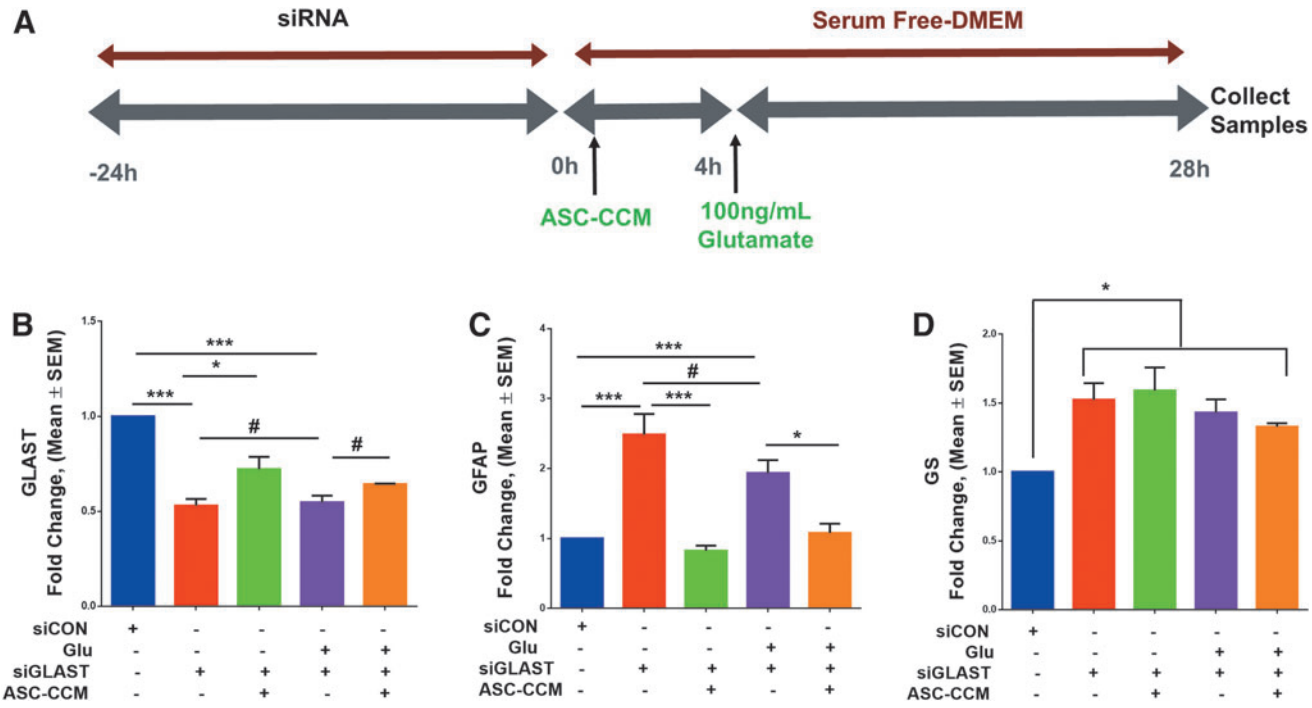

FIG. 11. ASC-CCM alleviates glutamate induced gliosis through actions on glutamate-aspartate transporter (GLAST) in Müller glia. **(A)** The schematic diagram of GLAST transfection in the rMC-1 cells. The rMC-1 cells were transfected with a GLAST small interfering RNA (siRNA) or a scrambled control siRNA (siCON). Assessment of gene expression by TaqMan quantitative polymerase chain reaction (qPCR)and expressed as fold change normalized to internal control (glyceraldehyde 3-phosphate dehydrogenase). **(B)** GLAST (***$p < 0.001$; *$p < 0.03$), **(C)** glial fibrillary acidic protein (GFAP; ***$p < 0.001$) and **(D)** glutamine synthetase (GS; *$p < 0.04$). # denotes $p > 0.05$. Data represent mean ± standard error of the mean (SEM) from $n = 3$ independent assessments /group. Color image is available online.

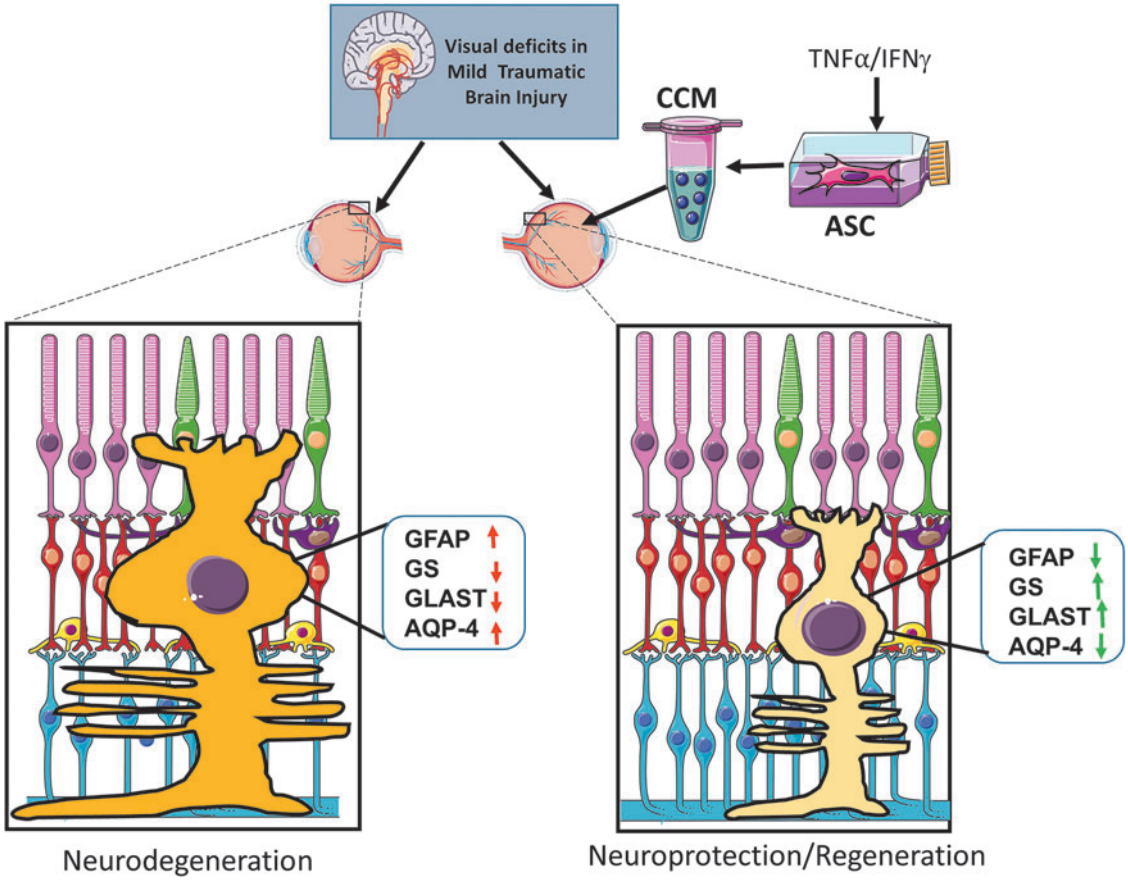

FIG. 12. The schematic model of ASC-CCM protects against visual deficits in mild traumatic brain injury model through improved Müller cell function via normalization of glial fibrillary acidic protein (GFAP), glutamine synthetase (GS), glutamate-aspartate transporter (GLAST), and aquaporin-4 (AQP4) expression in the retina. Created with content from Servier Medical Art (https://smart.servier.com) under CreativeCommons Attribution 3.0 Unported license (https://creativecommons.org/licenses/by/3.0). Color image is available online.

findings highlight Müller cells as cellular and molecular targets for adult stem cell therapies in mTBI.

One feature of our study is the partial improvement in b-wave response with ASC-CCM after TBI, as assessed by ERG. It may be that ASC-CCM delivery is unable to completely reverse the injury, either because of an inherent limitation of any effort to reverse the aftermath of a neurotrauma, or because of some insufficiency in the dose, delivery mode or timing of the ASC-CCM administration. Additionally, human proteins in ASC-CCM may have limited interaction with mouse targets and the array of cells in the retina that are responsible for ERG response. Further studies are needed to relate the changes observed here in Müller cell function to the TBI-induced retinal injury and functional deficits to better understand the therapeutic actions of ASC-CCM. Nonetheless, our results suggest that developing better secretome-derived biologics to stimulate endogenous repair and regeneration acting via multiple cell types in the retina promises to revolutionize treatments for visual deficits of mTBI.

Funding Information

This study was funded by grants from the Department of Defense (W81XWH-16-1-0761), National Eye Institute (EY023427), and unrestricted funds from Research to Prevent Blindness to R.G and Department of Defense (W81XWH-16-1-0076) to AR. KAJ is a recipient of a post-doctoral fellowship award from the Neuroscience Institute, UTHSC. The funders played no role in the conduct of the study, collection of data, management of the study, analysis of data, interpretation of data, or preparation of the manuscript.

Author Disclosure Statement

NS and RG are co-founders and hold equity in Cell Care Therapeutics Inc., whose interest is in the use of adipose-derived stromal cells in visual disorders.

For the other authors, no competing financial interests exist.

References

1. Guley, N.H., Rogers, J.T., Del Mar, N.A., Deng, Y., Islam, R.M., D'Surney, L., Ferrell, J., Deng, B., Hines-Beard, J., Bu, W., Ren, H., Elberger, A.J., Marchetta, J.G., Rex, T.S., Honig, M.G., and Reiner, A. (2016). A novel closed-head model of mild traumatic brain injury using focal primary overpressure blast to the cranium in mice. J. Neurotrauma 33, 403–422.
2. Mammadova, N., Ghaisas, S., Zenitsky, G., Sakaguchi, D.S., Kanthasamy, A.G., Greenlee, J.J., and West Greenlee, M.H. (2017). Lasting retinal injury in a mouse model of blast-induced trauma. Am. J. Pathol. 187, 1459–1472.
3. Bringmann, A., Iandiev, I., Pannicke, T., Wurm, A., Hollborn, M., Wiedemann, P., Osborne, N.N., and Reichenbach, A. (2009). Cellular signaling and factors involved in Muller cell gliosis: neuroprotective and detrimental effects. Prog. Retin Eye Res. 28, 423–451.
4. Bringmann, A., Pannicke, T., Grosche, J., Francke, M., Wiedemann, P., Skatchkov, S.N., Osborne, N.N., and Reichenbach, A. (2006). Muller cells in the healthy and diseased retina. Prog. Retin. Eye Res. 25, 397–424.
5. Delyfer, M.N., Forster, V., Neveux, N., Picaud, S., Léveillard, T., and Sahel, J.A. (2005). Evidence for glutamate-mediated excitotoxic mechanisms during photoreceptor degeneration in the rd1 mouse retina. Mol. Vis. 11, 688–696.
6. Ambati, J., Chalam, K.V., Chawla, D.K., D'Angio, C.T., Guillet, E.G., Rose, S.J., Vanderlinde, R.E., and Ambati, B.K. (1997). Elevated gamma-aminobutyric acid, glutamate, and vascular endothelial growth factor levels in the vitreous of patients with proliferative diabetic retinopathy. Arch. Ophthalmol. 115, 1161–1166.
7. Martin, K.R., Levkovitch-Verbin, H., Valenta, D., Baumrind, L., Pease, M.E., and Quigley, H.A. (2002). Retinal glutamate transporter changes in experimental glaucoma and after optic nerve transection in the rat. Invest. Ophthalmol. Vis. Sci. 43, 2236–2243.
8. Derouiche, A. (1996). Possible role of the Muller cell in uptake and metabolism of glutamate in the mammalian outer retina. Vision Res. 36, 3875–3878.
9. Linser, P. and Moscona, A.A. (1979). Induction of glutamine synthetase in embryonic neural retina: localization in Muller fibers and dependence on cell interactions. Proc. Natl. Acad. Sci. U. S. A. 76, 6476–6480.
10. Gorovits, R., Yakir, A., Fox, L.E., and Vardimon, L. (1996). Hormonal and non-hormonal regulation of glutamine synthetase in the developing neural retina. Brain Res. Mol. Brain Res. 43, 321–329.
11. Shaked, I., Ben-Dror, I., and Vardimon, L. (2002). Glutamine synthetase enhances the clearance of extracellular glutamate by the neural retina. J. Neurochem. 83, 574–580.
12. Li, J., Patil, R.V., and Verkman, A.S. (2002). Mildly abnormal retinal function in transgenic mice without Muller cell aquaporin-4 water channels. Invest. Ophthalmol. Vis. Sci. 43, 573–579.
13. Jha, K.A., Nag, T.C., Kumar, V., Kumar, P., Kumar, B., Wadhwa, S., and Roy, T.S. (2015). Differential Expression of AQP1 and AQP4 in Avascular Chick Retina Exposed to Moderate Light of Variable Photoperiods. Neurochem. Res. 40, 2153–2166.
14. Iandiev, I., Pannicke, T., Reichenbach, A., Wiedemann, P., and Bringmann, A. (2007). Diabetes alters the localization of glial aquaporins in rat retina. Neurosci. Lett. 421, 132–136.
15. Mead, B. and Tomarev, S. (2020). Extracellular vesicle therapy for retinal diseases. Prog. Retin. Eye Res, 100849.
16. Jha, K.A., Pentecost, M., Lenin, R., Klaic, L., Elshaer, S.L., Gentry, J., Russell, J.M., Beland, A., Reiner, A., Jotterand, V., Sohl, N., and Gangaraju, R. (2018). Concentrated conditioned media from adipose tissue derived mesenchymal stem cells mitigates visual deficits and retinal inflammation following mild traumatic brain injury. Int. J. Mol. Sci. 19.
17. Jha, K.A., Pentecost, M., Lenin, R., Gentry, J., Klaic, L., Del Mar, N., Reiner, A., Yang, C.H., Pfeffer, L.M., Sohl, N., and Gangaraju, R. (2019). TSG-6 in conditioned media from adipose mesenchymal stem cells protects against visual deficits in mild traumatic brain injury model through neurovascular modulation. Stem Cell Res. Therapy 10, 318.
18. Honig, M.G., Del Mar, N.A., Henderson, D.L., Ragsdale, T.D., Doty, J.B., Driver, J.H., Li, C., Fortugno, A.P., Mitchell, W.M., Perry, A.M., Moore, B.M., and Reiner, A. (2019). Amelioration of visual deficits and visual system pathology after mild TBI via the cannabinoid Type-2 receptor inverse agonism of raloxifene. Exp. Neurol. 322, 113063.
19. Verkman, A.S., Ruiz-Ederra, J., and Levin, M.H. (2008). Functions of aquaporins in the eye. Prog. Retin. eye res. 27, 420–433.
20. Honig, M.G., Del Mar, N.A., Henderson, D.L., Ragsdale, T.D., Doty, J.B., Driver, J.H., Li, C., Fortugno, A.P., Mitchell, W.M., Perry, A.M., Moore, B.M., and Reiner, A. (2019). Amelioration of visual deficits and visual system pathology after mild TBI via the cannabinoid Type-2 receptor inverse agonism of raloxifene. Exp. Neurol. 322, 113063.
21. Ulshafer, R.J., Sherry, D.M., Dawson, R. Jr., and Wallace, D.R. (1990). Excitatory amino acid involvement in retinal degeneration. Brain Res. 531, 350–354.
22. Bringmann, A., Pannicke, T., Grosche, J., Francke, M., Wiedemann, P., Skatchkov, S.N., Osborne, N.N., and Reichenbach, A. (2006). Müller cells in the healthy and diseased retina. Prog. Retin. Eye Res. 25, 397–424.
23. Louzada-Junior, P., Dias, J.J., Santos, W.F., Lachat, J.J., Bradford, H.F., and Coutinho-Netto, J. (1992). Glutamate release in experimental ischaemia of the retina: an approach using microdialysis. J. Neurochem. 59, 358–363.
24. Wang, L., Deng, Q.Q., Wu, X.H., Yu, J., Yang, X.L., and Zhong, Y.M. (2013). Upregulation of glutamate-aspartate transporter by glial cell line-derived neurotrophic factor ameliorates cell apoptosis in neural retina in streptozotocin-induced diabetic rats. CNS Neurosci. Ther. 19, 945–953.
25. Holcombe, D.J., Lengefeld, N., Gole, G.A., and Barnett, N.L. (2008). The effects of acute intraocular pressure elevation on rat retinal glutamate transport. Acta Ophthalmol. 86, 408-414.
26. Ginsberg, S.D., Martin, L.J., and Rothstein, J.D. (1995). Regional deafferentation down-regulates subtypes of glutamate transporter proteins. J. Neurochem. 65, 2800–2803.

27. Rao, V.L., Başkaya, M.K., Doğan, A., Rothstein, J.D., and Dempsey, R.J. (1998). Traumatic brain injury down-regulates glial glutamate transporter (GLT-1 and GLAST) proteins in rat brain. J. Neurochem. 70, 2020–2027.
28. Sullivan, S.M., Lee, A., Björkman, S.T., Miller, S.M., Sullivan, R.K., Poronnik, P., Colditz, P.B., and Pow, D.V. (2007). Cytoskeletal anchoring of GLAST determines susceptibility to brain damage: an identified role for GFAP. J. Biol. Chem. 282, 29414–29423.
29. Petito, C.K., Chung, M.C., Verkhovsky, L.M., and Cooper, A.J. (1992). Brain glutamine synthetase increases following cerebral ischemia in the rat. Brain Res. 569, 275–280.
30. Manogaran, P., Samardzija, M., Schad, A.N., Wicki, C.A., Walker-Egger, C., Rudin, M., Grimm, C., and Schippling, S. (2019). Retinal pathology in experimental optic neuritis is characterized by retrograde degeneration and gliosis. Acta Neuropathol. Commun. 7, 116.
31. Koh, S., Chen, W.J., Dejneka, N.S., Harris, I.R., Lu, B., Girman, S., Saylor, J., Wang, S., and Eroglu, C. (2018). Subretinal human umbilical tissue-derived cell transplantation preserves retinal synaptic connectivity and attenuates Müller glial reactivity. J. Neurosci. 38, 2923–2943.
32. Koh, S., Kim, N., Yin, H.H., Harris, I.R., Dejneka, N.S., and Eroglu, C. (2015). Human umbilical tissue-derived cells promote synapse formation and neurite outgrowth via thrombospondin family proteins. J. Neurosci. 35, 15649–15665.
33. Iandiev, I., Wurm, A., Hollborn, M., Wiedemann, P., Grimm, C., Reme, C.E., Reichenbach, A., Pannicke, T., and Bringmann, A. (2008). Muller cell response to blue light injury of the rat retina. Invest. Ophthalmol. Vis. Sci. 49, 3559–3567.
34. Buchi, E.R. (1992). Cell death in the rat retina after a pressure-induced ischaemia-reperfusion insult: an electron microscopic study. I. Ganglion cell layer and inner nuclear layer. Exp. Eye Res. 55, 605–613.
35. Kuroiwa, S., Katai, N., Shibuki, H., Kurokawa, T., Umihira, J., Nikaido, T., Kametani, K., and Yoshimura, N. (1998). Expression of cell cycle-related genes in dying cells in retinal ischemic injury. Invest. Ophthalmol. Vis. Sci. 39, 610–617.
36. de Vitry, F., Picart, R., Jacque, C., and Tixier-Vidal, A. (1981). Glial fibrillary acidic protein. A cellular marker of tanycytes in the mouse hypothalamus. Dev. Neurosci. 4, 457–460.
37. Fukuda, M., Nakanishi, Y., Fuse, M., Yokoi, N., Hamada, Y., Fukagawa, M., Negi, A., and Nakamura, M. (2010). Altered expression of aquaporins 1 and 4 coincides with neurodegenerative events in retinas of spontaneously diabetic Torii rats. Exp. Eye Res. 90, 17–25.
38. Bringmann, A. and Wiedemann, P. (2012). Müller glial cells in retinal disease. Ophthalmologica 227, 1–19.
39. Dharmarajan, S., Gurel, Z., Wang, S., Sorenson, C.M., Sheibani, N., and Belecky-Adams, T.L. (2014). Bone morphogenetic protein 7 regulates reactive gliosis in retinal astrocytes and Müller glia. Mol. Vis. 20, 1085–1108.
40. Wang, H., Song, G., Chuang, H., Chiu, C., Abdelmaksoud, A., Ye, Y., and Zhao, L. (2018). Portrait of glial scar in neurological diseases. Int. J. Immunopathol. Pharmacol. 31, 2058738418801406.
41. Nielsen, S., Nagelhus, E.A., Amiry-Moghaddam, M., Bourque, C., Agre, P., and Ottersen, O.P. (1997). Specialized membrane domains for water transport in glial cells: high-resolution immunogold cytochemistry of aquaporin-4 in rat brain. J. Neurosci. 17, 171–180.
42. Papadopoulos, M.C. and Verkman, A.S. (2007). Aquaporin-4 and brain edema. Pediatr. Nephrol. 22, 778–784.
43. Oosuka, S., Kida, T., Oku, H., Horie, T., Morishita, S., Fukumoto, M., Sato, T., and Ikeda, T. (2020). Effects of an aquaporin 4 inhibitor, TGN-020, on murine diabetic retina. Int. J. Mol. Sci. 21.
44. Zou, Y.Y., Kan, E.M., Lu, J., Ng, K.C., Tan, M.H., Yao, L., and Ling, E.A. (2013). Primary blast injury-induced lesions in the retina of adult rats. J. Neuroinflammation 10, 79.
45. Da, T. and Verkman, A.S. (2004). Aquaporin-4 gene disruption in mice protects against impaired retinal function and cell death after ischemia. Invest. Ophthalmol. Vis. Sci. 45, 4477–4483.
46. Li, J. and Verkman, A.S. (2001). Impaired hearing in mice lacking aquaporin-4 water channels. J. Biol. Chem. 276, 31233–31237.
47. Li, X.M., Wendu, R.L., Yao, J., Ren, Y., Zhao, Y.X., Cao, G.F., Qin, J., and Yan, B. (2014). Abnormal glutamate metabolism in the retina of aquaporin 4 (AQP4) knockout mice upon light damage. Neurol. Sci. 35, 847–853.

Address correspondence to:
Rajashekhar Gangaraju, PhD
Department of Ophthalmology, Anatomy, and Neurobiology
Neuroscience Institute
University of Tennessee Health Science Center
930 Madison Avenue Suite 768
Memphis, TN 38163
USA

E-mail: sgangara@uthsc.edu